Temporal contrast enhancement of femtosecond pulses by a self-diffraction process in a bulk Kerr medium

Jun Liu,[1,2,3,*] Kotaro Okamura,[1,2] Yuichiro Kida,[1,2] and Takayoshi Kobayashi[1,2,4,5]

[1] *Advanced Ultrafast Laser Research Center, University of Electro-Communications, Chofugaoka 1-5-1, Chofu, Tokyo 182-8585 Japan*
[2] *International Cooperative Research Project (ICORP), Japan Science and Technology Agency, 4-1-8 Honcho, Kawaguchi, Saitama 332-0012, Japan*
[3] *State Key Laboratory of High Field Laser Physics, Shanghai Institute of Optics and Fine Mechanics, Chinese Academy of Sciences, Shanghai 201800, China*
[4] *Department of Electrophysics, National Chiao Tung University, 1001 Ta Hsueh Rd. Hsinchu 300, Taiwan*
[5] *Institute of Laser Engineering, Osaka University, Yamadakami 2-6, Suita 565-0871, Ibaraki 567-0047, Japan*
** jliu@ils.uec.ac.jp*

Abstract: We demonstrated for the first time the application of a self-diffraction (SD) process in a bulk Kerr medium to improve the temporal, spectral, and spatial qualities of femtosecond laser pulses. A proof-of-principle experiment succeeded in improving the temporal contrast of a femtosecond pulse by four orders of magnitude even in the picosecond region using a 0.5-mm-thick fused silica glass plate by this technique. The energy conversion efficiency from the incident pulses to the two first-order SD signals is about 12%. By the SD process, a laser pulse with smoother spectral shape, higher beam quality, and shorter pulse duration than those of the input pulse was generated. This technique is expected to be used to design background-free petawatt laser system in the future.

OCIS codes: (190.4380) Nonlinear optics, four-wave-mixing; (190. 4410) Nonlinear optics, parametric processes; (190.7110) Ultrafast nonlinear optics; (320.5520) Pulse compression.

References and links

1. H. Kiriyama, M. Mori, Y. Nakai, T. Shimomura, H. Sasao, M. Tanoue, S. Kanazawa, D. Wakai, F. Sasao, H. Okada, I. Daito, M. Suzuki, S. Kondo, K. Kondo, A. Sugiyama, P. R. Bolton, A. Yokoyama, H. Daido, S. Kawanishi, T. Kimura, and T. Tajima, "High temporal and spatial quality petawatt-class Ti:sapphire chirped-pulse amplification laser system," Opt. Lett. **35**(10), 1497–1499 (2010).
2. V. Yanovsky, V. Chvykov, G. Kalinchenko, P. Rousseau, T. Planchon, T. Matsuoka, A. Maksimchuk, J. Nees, G. Cheriaux, G. Mourou, and K. Krushelnick, "Ultra-high intensity- 300-TW laser at 0.1 Hz repetition rate," Opt. Express **16**(3), 2109–2114 (2008).
3. S. V. Bulanov, T. Esirkepov, D. Habs, F. Pegoraro, and T. Tajima, "Relativistic Laser-Matter Interaction and Relativistic Laboratory Astrophysics," Eur. Phys. J. D **55**(2), 483–507 (2009).
4. G. A. Mourou, T. Tajima, and S. V. Bulanov, "Optics in the relativistic regime," Rev. Mod. Phys. **78**(2), 309–371 (2006).
5. P. Antici, J. Fuchs, E. d'Humières, E. Lefebvre, M. Borghesi, E. Brambrink, C. A. Cecchetti, S. Gaillard, L. Romagnani, Y. Sentoku, T. Toncian, O. Willi, P. Audebert, and H. Pépin, "Energetic protons generated by ultrahigh contrast laser pulses interacting with ultrathin targets," Phys. Plasmas **14**(3), 030701–1 (2007).
6. B. Dromey, M. Zepf, A. Gopa, K. Lancaster, M. S. Wei, K. Krushelnick, M. Tatarakis, N. Vakakis, S. Moustaizis, R. Kodama, M. Tampo, C. Stoeck, R. Clarke, H. Habara, D. Neely, S. Karsch, and P. Norreys, "High harmonic generation in the relativistic limit," Nat. Phys. **2**(7), 456–459 (2006).
7. M. Nantel, J. Itatani, T. An-Chun, J. Faure, D. Kaplan, M. Bauvier, T. Buma, P. Van Rompay, J. Nee, P. P. Pronko, D. Umstadter, and G. A. Mourou, "Temporal contrast in Ti:sapphire lasers, characterization and control," IEEE J. Sel. Top. Quantum Electron. **4**(2), 449–458 (1998).
8. H. Kiriyama, M. Mori, Y. Nakai, Y. Yamamoto, M. Tanoue, A. Akutsu, T. Shimomura, S. Kondo, S. Kanazawa, H. Daido, T. Kimura, and N. Miyanaga, "High-energy, high-contrast, multiterawatt laser pulses by optical parametric chirped-pulse amplification," Opt. Lett. **32**(16), 2315–2317 (2007).
9. M. Kalashnikov, E. Risse, H. Schönnagel, A. Husakou, J. Herrmann, and W. Sandner, "Characterization of a nonlinear filter for the front-end of a high contrast double-CPA Ti:sapphire laser," Opt. Express **12**(21), 5088–5097 (2004).

#132521 - $15.00 USD Received 2 Aug 2010; revised 5 Sep 2010; accepted 7 Sep 2010; published 6 Oct 2010

10. M. P. Kalashnikov, E. Risse, H. Schönnagel, and W. Sandner, "Double chirped-pulse-amplification laser: a way to clean pulses temporally," Opt. Lett. **30**(8), 923–925 (2005).
11. V. Chvykov, P. Rousseau, S. Reed, G. Kalinchenko, and V. Yanovsky, "Generation of 10(^{11}) contrast 50 TW laser pulses," Opt. Lett. **31**(10), 1456–1458 (2006).
12. J. Itatani, J. Faure, M. Nantel, G. Mourou, and S. Watanabe, "Suppression of the amplified spontaneous emission in chirped-pulse-amplification lasers by clean high-energy seed-pulse injection," Opt. Commun. **148**(1-3), 70–74 (1998).
13. A. Renault, F. Augé-Rochereau, T. Planchon, P. Doliveira, T. Auguste, G. Cheriaux, and J. Chambaret, "ASE contrast improvement with a non-linear filtering Sagnac interferometer," Opt. Commun. **248**(4-6), 535–541 (2005).
14. G. Doumy, F. Quéré, O. Gobert, M. Perdrix, P. Martin, P. Audebert, J.-C. Gauthier, J.-P. Geindre, and T. Wittmann, "Complete characterization of a plasma mirror for the production of high-contrast ultraintense laser pulses," Phys. Rev. E Stat. Nonlin. Soft Matter Phys. **69**(2), 026402–1 (2004).
15. D. Homoelle, A. L. Gaeta, V. Yanovsky, and G. Mourou, "Pulse contrast enhancement of high-energy pulses by use of a gas-filled hollow waveguide," Opt. Lett. **27**(18), 1646–1648 (2002).
16. A. Jullien, F. Augé-Rochereau, G. Chériaux, J. P. Chambaret, P. d'Oliveira, T. Auguste, and F. Falcoz, "High-efficiency, simple setup for pulse cleaning at the millijoule level by nonlinear induced birefringence," Opt. Lett. **29**(18), 2184–2186 (2004).
17. A. Jullien, O. Albert, F. Burgy, G. Hamoniaux, J.-P. Rousseau, J.-P. Chambaret, F. Augé-Rochereau, G. Chériaux, J. Etchepare, N. Minkovski, and S. M. Saltiel, "10(-10) temporal contrast for femtosecond ultraintense lasers by cross-polarized wave generation," Opt. Lett. **30**(8), 920–922 (2005).
18. A. Cotel, A. Jullien, N. Forget, O. Albert, G. Cheriaux, and C. Le Blanc, "Nonlinear temporal pulse cleaning of a 1-mu m optical parametric chirped-pulse amplification system," Appl. Phys. B **83**(1), 7–10 (2006).
19. K. W. DeLong, R. Trebino, and D. J. Kane, "Comparison of ultrashort-pulse frequency-resolved-optical-gating traces for three common beam geometries," J. Opt. Soc. Am. B **11**(9), 1595–1608 (1994).
20. T. S. Clement, A. J. Taylor, and D. J. Kane, "Single-shot measurement of the amplitude and phase of ultrashort laser pulses in the violet," Opt. Lett. **20**(1), 70–72 (1995).
21. R. Trebino, Frequency-Resolved Optical Grating: The Measurement of Ultrashort Laser Pulses, (Kluwer Academic Publishers) (2000).
22. J. Liu, and T. Kobayashi, "Generation and amplification of tunable multicolored femtosecond laser pulses by using cascaded four-wave mixing in transparent bulk media," Sensors **10**, 4296–4341 (2010). *http://www.mdpi.com/1424-8220/10/5/4296/pdf*.
23. T. Schneider, D. Wolfframm, R. Mitzner, and J. Reif, "Ultrafast optical switching by instantaneous laser-induced grating formation and self-diffraction in barium fluoride," Appl. Phys. B **68**(4), 749–751 (1999).
24. K. W. DeLong, R. Trebino, J. Hunter, and W. E. White, "Frequency-resolved optical gating with the use of second-harmonic generation," J. Opt. Soc. Am. B **11**(11), 2206–2215 (1994).
25. A. Jullien, L. Canova, O. Albert, D. Boschetto, L. Antonucci, Y. H. Cha, J. P. Rousseau, P. Chaudet, G. Cheriaux, J. Etchepare, S. Kourtev, N. Minkovski, and S. M. Saltiel, "Spectral broadening and pulse duration reduction during cross-polarized wave generation: influence of the quadratic spectral phase," Appl. Phys. B **87**(4), 595–601 (2007).
26. X. W. Chen, Y. X. Leng, J. Liu, Y. Zhu, R. X. Li, and Z. Z. Xu, "Pulse self-compression in normally dispersive bulk media," Opt. Commun. **259**(1), 331–335 (2006).
27. J. Liu, X. W. Chen, J. S. Liu, Y. Zhu, Y. X. Leng, J. Dai, R. X. Li, and Z. Z. Xu, "Spectrum reshaping and pulse self-compression in normally dispersive media with negatively chirped femtosecond pulses," Opt. Express **14**(2), 979–987 (2006).
28. G. Pretzler, A. Kasper, and K. J. Witte, "Angular chirp and tilted light pulses in CPA lasers," Appl. Phys. B **70**(1), 1–9 (2000).
29. K. Osvay, A. P. Kovács, Z. Heiner, G. Kurdi, J. Klebniczki, and M. Csatári, "Angular dispersion and temporal change of femtosecond pulse from misaligned pulse compressors," IEEE J. Sel. Top. Quantum Electron. **10**(1), 213–220 (2004).
30. T. J. Wang, Z. Major, I. Ahmad, S. A. Trushin, F. Krausz, and S. Karsch, "Ultrabroadband near-infrared pulse generation by noncollinear OPA with angular dispersion compensation," Appl. Phys. B **100**(1), 207–214 (2010).
31. O. Gilbert, C. Deumié, and C. Amra, "Angle-resolved ellipsometry of scattering patterns from arbitrary surfaces and bulks," Opt. Express **13**(7), 2403–2418 (2005).
32. H. H. Hou, K. Yi, S. Z. Shang, J. D. Shao, and Z. X. Fan, "Measurements of light scattering from glass substrates by total integrated scattering," Appl. Opt. **44**(29), 6163–6166 (2005).

1. Introduction

Owning to the great progress in chirped-pulse amplification (CPA) technique, a petawatt-class laser system has been developed [1] and laser intensity has recently reached a level as high as 10^{22} W/cm^2 [2]. Such ultrahigh intense laser pulses provide powerful tools for laser-matter interaction experiments in the relativistic regime [3,4]. In these plasma-creating experiments, laser pulses with high temporal contrast are required to prevent the unwanted intense prepulses which generate preplasma before the main pulse arrives at the target [5,6]. For laser intensity as high as 10^{21} W/cm^2, it is of vital importance to increase the pulse contrast better

#132521 - $15.00 USD Received 2 Aug 2010; revised 5 Sep 2010; accepted 7 Sep 2010; published 6 Oct 2010

than 10^9 to prevent the generation of preplasma. However, the temporal contrast of a typical CPA system can only reach 10^6 of the magnitude [7]. To improve the temporal contrast of this extremely intense femtosecond pulse, optical parametric chirped pulse amplification (OPCPA) and double CPA systems were widely used [1,2,8–11]. Furthermore, several pulse-cleaning techniques have been developed to improve the temporal contrast. These methods include the use of saturable absorbers [1,12], a nonlinear Sagnac interferometer [13], plasma mirrors [14], polarization rotation [9,15,16], and cross-polarized wave (XPW) generation [2,11,17,18]. However, in the case of the first three methods, the temporal contrast improvement is limited to only 1-3 orders of magnitude. Plasma mirrors can only be used under the condition of low repetition rates due to the plasma lifetime. Recently, polarization rotation and XPW, based on the third-order nonlinear process, were demonstrated as powerful methods to improve the temporal contrast of intense laser pulses. By using XPW in BaF_2 crystals, the temporal contrast has been improved by about four orders of magnitude [2,11,17,18]. In these two methods, the contrast enhancement has been limited by the extinction ratio of the polarization discrimination device which is at best 4-5 orders [15–18].

In this letter, we demonstrated for the first time using another third-order nonlinear process, self-diffraction (SD) process, to improve the temporal contrast of a femtosecond laser pulse. The advantage of this method is that the generated SD signals are spatially separated from incident beams without any need of polarization discrimination device. It was proved that the temporal contrast can be improved by four orders of magnitude by this technique even in the picosecond regime for the first-order SD signal. The analysis indicated that the diffusive light from the Kerr medium and the angular dispersion are the two main obstacles of the enhancement of temporal contrast in the method. It was also found that the laser spectrum was smoothed and broadened together with the reduction of the pulse duration, and furthermore the spatial quality of the beam was improved in this process.

2. Principle

SD process was studied and used to measure the pulse duration about a decade ago [19–21]. For the SD process, two incident pulses have the same wavelengths, thus it can be called degenerate cascaded four-wave mixing process. The same as cascaded four-wave mixing (CFWM) process [22], this third-order nonlinear optical parametric process needs phase-matching condition: $k_{sd\pm m} = (m+1)k_{\pm 1} - mk_{\mp 1}$ and $\omega_{sd\pm m} = (m+1)\omega_{\pm 1} - m\omega_{\mp 1}$, where, $\boldsymbol{k}$ is the wave vector, w is the angular frequency, and m is the SD order number, which is schematically shown in Fig. 1a. From the phase-matching condition, the generated SD signals have almost the same center wavelength with the incident pulse. As the first-order SD (referred to henceforth as SD1) process is a third-order nonlinear process, the intensity of the first-order SD signal has a cubic dependence on the intensity of the incident pulse. The third-order nonlinear response inducing SD1 in transparent materials is purely electronic and hence instantaneous in the non-resonant condition. The intensity of SD1 can be expressed simply as: $I_{sd1} \propto I_1^2(t) I_{-1}(t-\tau)$ in time domain. In a non-resonant electronic Kerr medium, the SD process is an instantaneous process with femtosecond time scale because of inertia-free interaction [23]. The weak amplified spontaneous emission (ASE) with long life time and satellite pulses will experience SD processes separated from the main pulse in time. Moreover, by using SD process, the SD signals are spatially separated from the two input beams. Therefore there is no limit of improvement of temporal contrast due to the extinction ratio of the polarizer pair like XPW generation method. If the angular dispersion is not taken into consideration and the diffusive light from the Kerr medium is negligibly small in comparison with the noise in the SD pulse, the temporal contrast of the SD1 signal can be estimated as the cube of the temporal contrast of incident pulses $C_{sd1} \approx (C_{in})^3$ even in the picosecond range. Furthermore, the higher order SD signals have a much higher temporal contrast improvement from the relations: $I_{sd(m+1)} \propto I_1^{m+2}(t) I_{-1}^{m+1}(t-\tau)$. The time-domain expression also indicates that the pulse duration of the SD1 signal will be shortened in the SD

#132521 - $15.00 USD Received 2 Aug 2010; revised 5 Sep 2010; accepted 7 Sep 2010; published 6 Oct 2010

process. In the frequency domain, the third-order dielectric polarization induced at a certain frequency ω_{sd1} is obtained by the sum over all possible permutations of fundamental frequencies weighted according to the third-order susceptibility. As a result, the intensity of the SD1 signal can be described as [21]:

$$I_{sd1}(\omega_{sd1}) \propto \left| \iint d\omega_1 d\omega_{-1} \chi^{(3)} \tilde{E}_1^*(z,\omega_1) \tilde{E}_{-1}(z,\omega_{-1}) \tilde{E}_1(z,\omega_{sd1}-\omega_{-1}+\omega_1) \sin c(\Delta k_z(\omega_{sd1},\omega_1,\omega_{-1})L/2) \right|^2$$

Here, ω_{sd1} and ω_1 and ω_{-1} are the angular frequencies of the SD1 signal, and the two incident beams, respectively. $\Delta k_z(\omega_{sd1},\omega_1,\omega_{-1})$ is the phase mismatch, L is the path length in the medium. As one can see, the spectral intensity of the SD1 signal is an integral of the spectral intensity of two incident laser pulses. It means that the intensity of the SD1 signal at every wavelength component is an averaged contribution over the whole spectral region of the incident pulses. Therefore, the spectrum of the SD1 signal is smoothed automatically. Moreover, this averaged contribution makes the central wavelength components to be suppressed and the weak wings on both sides to be enhanced. Simultaneously, from the phase-matching condition, new wavelength will be generated on the both sides of the SD1 signal spectrum. As a result, the spectrum of the SD1 signal is broadened. This SD process can be run in a wide spectral range with a broadband incident spectrum when the incident crossing angle is small and the thickness of the medium is thin enough based on the description in SD frequency-resolved optical gating (FROG) measurement [21].

3. Experimental setup

The experiment was performed with a commercial Ti:sapphire CPA laser system (Legend-USP, coherent). The laser system produced a pulse with the pulse duration of 35-fs, 2.5-mJ maximal pulse energy, a center wavelength of 800 nm, and a repetition rate of 1-kHz. After four 1-mm-thick fused silica beamsplitters with 80/20, 80/20, 80/20, and 50/50 reflection/transmission ratios, respectively, pulse with about 110 μJ pulse energy was used in the experiment, as shown in Fig. 1b. Then, after a variable neutral-density (VND) filter, the laser pulse was split into two beams by another 50/50 beamsplitter. The transmitted beam is beam_1.The time delay of the reflective beam (beam_-1) can be tuned by a motor-controlled stage with a 10-nm/step. The two beams were focused by a spherical mirror with a 300-mm focal length into a 0.5-mm-thick fused silica glass plate located about 20 mm after the focal point. The beam diameters on the glass plate were both about 360 μm at $1/e^2$. The external crossing angle between the two incident laser beams was about 1.5°. Then, the phase matching condition can be easily satisfied. The individual transmission pulse energy of beam_1 and beam_-1 after the glass plate was 40 and 51 μJ, respectively. When the two beams were temporally synchronized and spatially overlapped in the glass plate, SD signals were appeared on the both sides besides the input beams. The pulse energies of the SD1 signals generated besides beam 1 and beam_-1 were about 5 and 6 μJ, respectively. The energy conversion efficiency from the input laser beams to the two SD1 signals was about 12%. The pulse energies of the SD2 signals were about 0.6 and 0.7 μJ on the sides of beam_1 and beam_-1, respectively. The efficiency on one of the two sides can be increased by replacing the 50/50 beamsplitter with a 67/33 beamsplitter to make the incident pulse energy ratio is 2:1. The ratios of the pulse energies between SD1 and SD2 signals can also be changed by tuning the incident crossing angle [22].

#132521 - $15.00 USD Received 2 Aug 2010; revised 5 Sep 2010; accepted 7 Sep 2010; published 6 Oct 2010

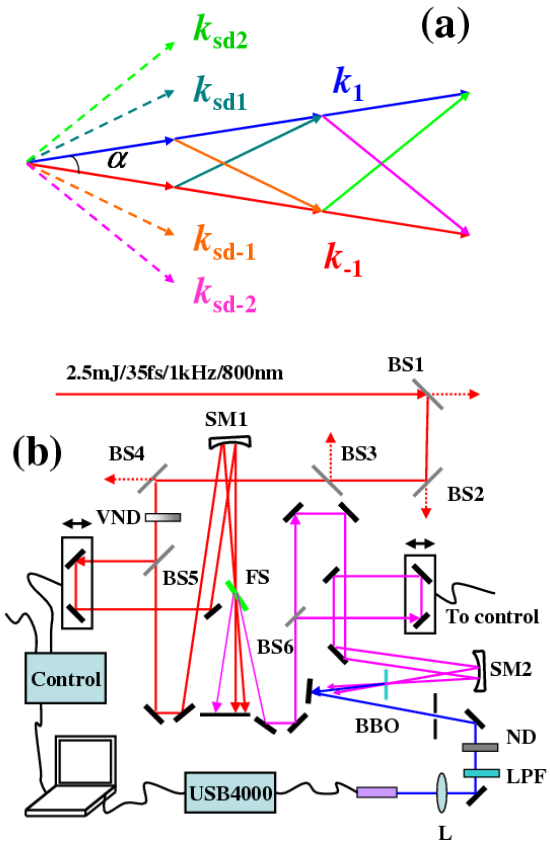

Fig. 1. (Color online) (a) Phase-matching geometry for self-diffraction process. a is the incident crossing angle. k1, k-1, k_{sdj1} and k_{sdj2} are wavevectors of the two incident beams and the generated first-order and second-order self-diffraction signals, respectively. (b) Experimental setup. BS1 to BS6 are six fused silica beamsplitters of 1-mm-thickness with 80/20, 80/20, 80/20, 50/50, 50/50, and 50/50 reflection/transmission ratios, respectively. VND: variable neutral-density filter. SM1: spherical mirror R = –600 mm. FS: 0.5-mm-thick fused silica glass plate. SM2: spherical mirror R = –500 mm. BBO: 70-μm-thick (Type I, θ = 29.2°). ND: 1000-times-reduction neutral-density filter. LPF: a short-wavelength-pass filter cutting at 440 nm. L: CaF_2 focusing lens with a focal length of f = 50 mm.

Due to the low pulse energy and low power level of the generated SD signals, we could not measure their high-dynamic range third-order correlation. To obtain the information of the pulse contrast, we performed a second-order autocorrelation measurement (SAC) which needs much lower incident pulse energy and is more sensitive to the low energy noise than other measurement techniques using third-order nonlinearity because it involves only one second-order nonlinearity [21,24]. Nearly the whole SD beam was guided into the SAC measurement to increase the dynamic range of the pulse contrast measurement. The only disadvantage of SAC is indistinguishability between a prepulse and a postpulse. However, we know from the principle above that the SD process is a Kerr induced gating process which will clean both the prepulse and the postpulse simultaneously. To prove this, we introduced prepulses by placing the non-coating surface of the 50/50 beamsplitter (BS4) on the front to reflect the light and the coating surface on the back. All the other beamsplitters were located in the opposite way that will introduce postpulses. In the SAC measurement, one more 1-mm-thick 50/50 beamsplitter was used to split the laser beam. The motor-controlled delay stage has a 10-nm/step resolution and a ± 10 mm maximal travel distance. A 70-μm-thick β–barium borate (BBO, Type I, θ = 29.2°) crystal was used to generate a sum-frequency (SF) signal. After passing through an aperture, a short-wavelength-pass filter cutting at 440 nm, and a 1000-times-reduction neutral-

#132521 - $15.00 USD Received 2 Aug 2010; revised 5 Sep 2010; accepted 7 Sep 2010; published 6 Oct 2010

density (ND) filter, the SF signal was focused into a fiber of 600 μm inner diameter and detected by a multi-channel spectrometer (USB4000, Ocean Optics) with 100 ms integration time.

4. Experimental results and discussion

The intensity of the SF signal at every delay time step was obtained by integrating the measured spectral intensity over the spectral range only from 370 to 430 nm by USB4000 to reduce the noise intensity at other wavelengths. The delay time was scanned by a motor-controlled stage. When the SF signal is so strong that it saturates the spectrometer (from −100 to 100 fs for SD1 signal measurement and from −1000 to 1000 fs for the incident pulse measurement), the signal energy was decreased 1000-times by inserting a 1000-times-reduction ND-filter. In this way, the delay time dependent SF intensities of incident laser pulses and the SD1 signal were obtained. To show it more clearly in Fig. 2, the data were normalized to the main peak intensity.

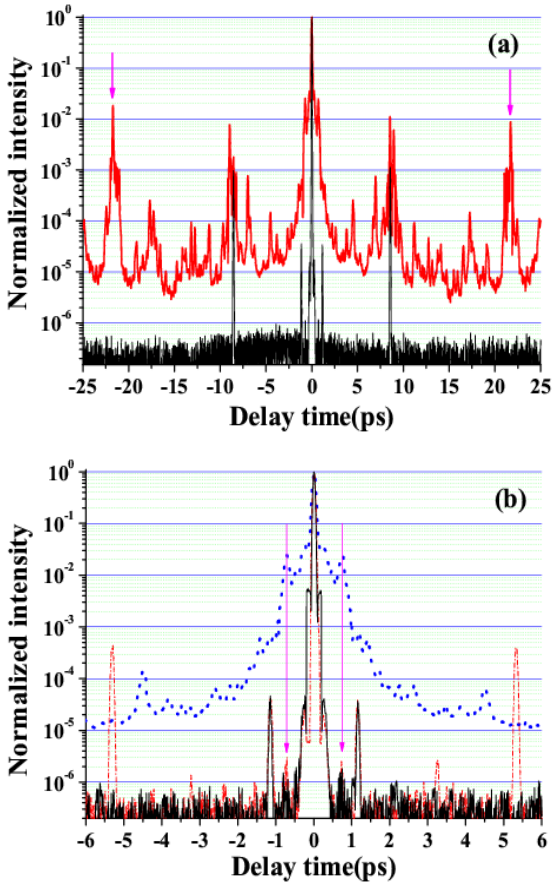

Fig. 2. (Color online) (a) SAC intensities of the incident pulse (upper red curve) and of the SD1 signal in the delay time from −25 to 25 ps and with a 10-fs/step resolution. (b) SAC intensities of the incident pulse (blue-dot curve) and SAC intensity of the SD1 signals when the glass was Brewster-angle located (black-solid curve) or was perpendicular located (red-dash-dot curve) to the incident beams in the delay time from −6 to 6 ps and with a 5-fs/step resolution.

Figure 2a shows the SAC intensity of the incident laser pulse and the SD1 signal in the delay time range from −25 to 25 ps with a 10-fs/step. It is very clear that the temporal contrast of the SD1 signal is improved from that of the incident pulses. The peak intensity of the most

#132521 - $15.00 USD Received 2 Aug 2010; revised 5 Sep 2010; accepted 7 Sep 2010; published 6 Oct 2010

intense noise locates around ± 21.8 ps, which is about the level of 10^{-2} of the peak intensity of the main pulse in the incident pulse. For the SD1 signal, it shows no peak at the same delay time. This means that the temporal contrast of the SD1 signal is improved to a value (10^6) that is the cube of that of the incident pulse (10^2) at this delay time. The contrast measurement of the SD1 signal is limited by the low energy of SD1 signal and the noise from the scattering of the bulk medium and the sensitivity of the spectrometer here. The two peaks at the SF intensity of the SD1 signal at about ± 8.7 and ± 1.1 ps are due to the back-and-front reflections by the beamsplitter and the 70-μm-thick BBO crystal used in the SAC, respectively. This is because the peaks at ± 1.1 ps delay were shifted when the thickness of the BBO crystal was changed and the peaks at ± 8.7 ps disappeared when the beamsplitter was replaced with a silver-coated D-shaped mirror. Figure 2b shows the data in the delay time range from –6 to 6 ps with a 5-fs/step. It is obvious that the pulse is cleaned even in the time range of one picosecond apart from the main pulse. The SAC peak intensity around ± 0.7 ps is about 1.2×10^{-2} of the main peak intensity in the incident pulse. The SAC of the SD1 signal shows that there is a small peak at the same delay with less than 1.2×10^{-6} of the peak intensity of the main pulse, which is improved by four orders of magnitude and is better than the cube of 1.2×10^{-2} (1.7×10^{-6}). Not only the self-diffraction itself but also the self-focusing effect contributes the improvement of the temporal contrast. In non-resonant electronic Kerr media, the self-focusing is also instantaneous and there is a power threshold due to the competition with the diffraction. The intensity dependent self-focusing effect increases the intensity of the main pulse while the ASE and the noise peaks are not enhanced. As a result, the much more increased intensity of the main pulse enhanced the self-diffraction process resulting in the further improvement of the temporal contrast. When the glass plate is located after the focal point, the generated SD1 signal has smaller divergence angle owing to the self-focusing process in comparison with the scattering light and then reduce the noise of the scattering light. In Fig. 2b (red dash-dot curve), the two peaks around ± 5.3 ps is the back-and-front reflected light by the 0.5-mm-thick glass of the main pulse when it was located nearly normal to the two incident beams. These peaks due to back and front reflection can be removed by locating the glass plate surfaces with the Brewster angle to the two incident beams, as shown in Fig. 2b with a black-solid curve.

The spectra of the SD1 signal and the input laser pulse are shown in Fig. 3a. The spectrum of the SD1 signal is clearly smoother and broader than the input laser spectrum. The pulse durations of the input pulse and the SD signal were measured by a SHG-FROG technique using the same setup as the temporal contrast measurement except for the 50/50 beamsplitter being replaced with a silver-coated D-shaped mirror to avoid the dispersion of the beamsplitter. All the data were retrieved by using the commercial software (FROG 3.0, Femtosoft Technologies) with retrieve errors smaller than 0.006. Figure 3a shows the retrieved incident-laser spectrum and retrieved SD1 spectrum with a thin magenta-dash-dot curve and a thin blue-dash-dot curve, respectively. The retrieved spectra fit well with the measured ones. Figure 3b shows that the pulse duration of the SD1 signal at zero delay time was shortened from 75 to 54 fs in comparison with the input pulse. The retrieved temporal and spectral phases in Figs. 3a and 3b show that the phase of the SD1 signal was also found to be smoothed with some positive chirp. Comparing with the spectrum of the SD1 signal at zero delay time, the peak wavelength of the SD1 signal was shifted for about ± 10 nm at ± 33 fs delay time (+ means beam_1 is ahead of beam_-1) owning to the cross phase modulation (XPM) and small frequency chirps of incident pulses [22], as shown in Fig. 3c. At the same delay time, the spectral-shifts of the two SD1 signals on both sides have opposite signs. The retrieved spectral phase also shows that the reduction or enhancement of the chirp rates depends on the sign of the delay time for the same SD1 signal, as shown in Fig. 3c. Suitable delay and chirp of the incident pulse will induce self-compression of the SD1 signal to a nearly transform-limited pulse. Figure 3b shows the temporal profile and temporal phase of the SD1 signal when the delay time is + 33 fs. The pulse duration was shortened to 39 fs, which is close to its transform-limited pulse duration 33 fs. These spectral broadening and

#132521 - $15.00 USD Received 2 Aug 2010; revised 5 Sep 2010; accepted 7 Sep 2010; published 6 Oct 2010

pulse shortening also appeared in another third-order nonlinear process, XPW generation [25], and they can be explained in almost the same way.

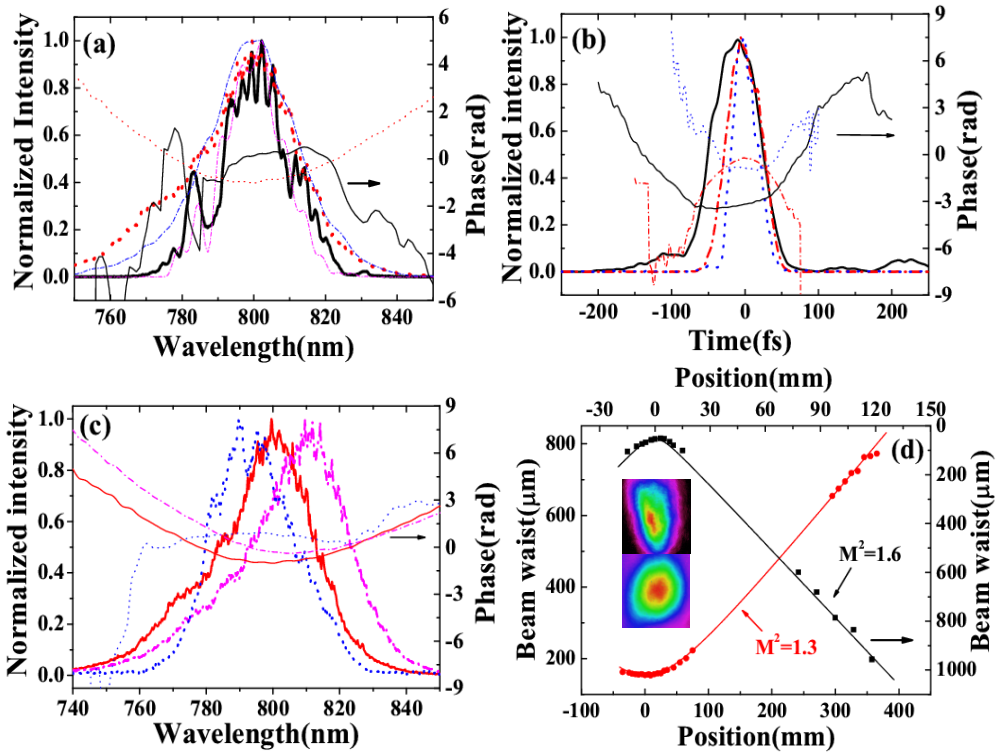

Fig. 3. (Color online) (a) Measured spectra (thick curve) and retrieved spectral phase (thin curve) of the incident pulse (black-solid curve) and the SD1 signal (red-dot curve).The thin blue-dash-dot curve and the thin magenta-dash-dot curve show the retrieved spectra of the SD1 and the incident pulse, respectively; (b) Retrieved temporal profile (thick curve) and temporal phase (thin curve) of the incident pulse (black-solid curve), the SD1 signals at zero (red-dash-dot curve) and at + 33 fs (blue-dot curve) delay time; (c) Measured spectra (thick curve) and retrieved spectral phase (thin curve) of the SD1 signals at zero (red-solid curve), –33 fs (magenta-dash-dot curve) and + 33 fs (blue-dot curve) delay time, respectively; (d) M^2 and two-dimensional beam profiles of the incident beam (black-square curve, up pattern) and the SD1 signal (red-circle curve, low pattern).

The spatial profile and beam quality of the SD1 signal were also improved in this SD process in comparison with the input laser beam owning to spatial filtering effect induced by self-focusing in the medium. This was observed in the same way in the CFWM experiments [22] and pulse compression experiments in bulk media [26,27]. The M^2 of the input laser beam and the SD1 signal were fitted by the beam diameters that measured using a CCD camera (BeamStar FX33, Ophir Optronics) at more than ten positions. The two dimensional beam profiles of the SD1 signal is improved from an asymmetric incident beam to a nearly-symmetric Gaussian beam, as illustrated in the inset pattern in Fig. 3d. The M^2 of the SD1 beam was also improved from 1.6 of the input laser beam to 1.3, as shown in Fig. 3d.

5. Influence of angular dispersion

SD process is a third-order nonlinear interaction in nonconllinear configuration and hence the generated SD signals are expected to have an angular chirp. The angular chirp was also shown in the CFWM signal in our previous work [22]. The SD1 beam was expanded to about 11 mm by an f = –200 mm negative lens and propagating for about 600 mm. We measured the spectra the SD1 beam at the three different positions, as shown in the inset of Fig. 4. C0 was the center measurement position. C5 and C-5 were the two positions 5 mm away from C0,

#132521 - $15.00 USD Received 2 Aug 2010; revised 5 Sep 2010; accepted 7 Sep 2010; published 6 Oct 2010

where C-5 is the one closer to the input beams. Longer wavelength located on the position far away from the two input beams and the shorter wavelength generated on the position close to the two incident beams. The center wavelength was shifted for about 15 nm between the two edge points C-5 and C5. From the measurement, it was roughly estimated that the angular dispersion was about 0.1mrad/nm. The angular dispersion will not affect the pulse duration at different point on the beam cross section. However, the angular dispersion leads to enlarge the focal spot and elongate the pulse at the focal point. As a result, it will reduce the focal intensity and affect the temporal contrast [28]. It will affect the compression of the pulse in the picosecond time region if it is not compensated. In a double-CPA scheme, it is expected to reduce the angular dispersion by the grating based stretcher after the SD process and then improve the temporal contrast after amplifier in the future [29]. A telescope-grating-deformable scheme is also proposed to compensate both the linear and the nonlinear angular dispersion of the parametric beam in this kind optical parametric laser system [30]. This improvement is expected to be done in the future.

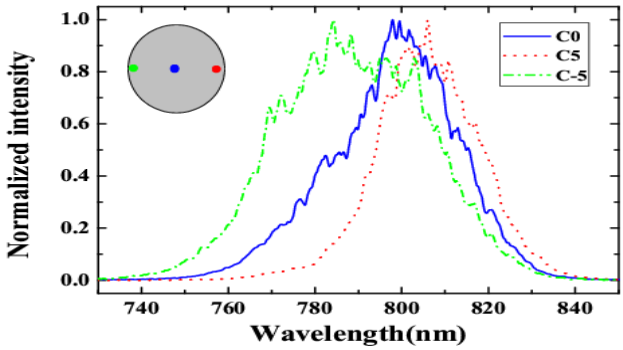

Fig. 4. (Color online) The SD spectra at the three different positions C0, C5, and C-5, respectively. The inset pattern shows the three different positions on the beam we measured. C0 is the center of the beam. C5 and C-5 refer to the two positions located about 5 mm from the center position C0. C-5 is the one closer to the incident beams.

6. Influence of scattering

From the above analysis, experiment, and discussion, it can be seen that the temporal contrast of a femtosecond laser pulse can be improved to the value higher than the cube of the temporal contrast in both prepulse and postpulse when the angular dispersion is neglected and the scattering from the Kerr medium is lower enough to be neglected.

In real system, the surface and the bulk of the bulk Kerr medium may suffer from finite scattering of the laser beams. Fortunately, the scattered light has a longer dwelling time than the main pulse. Then, these scattering lights from the main pulse will appear only as postpulses. For a bulk Kerr medium with small thickness (millimeter level), the scattered light is expected to appear within several picoseconds after the main pulse. This scattered light appeared in the postpulse will not affect the conventionally defined "temporal contrast" that only the prepulse is taken into account [1]. However, the scattering light from the satellite prepulses will affect the temporal contrast of the SD signal. It is possible to measure the relative scattered light in the signal direction by blocking one of the two input beams in the future. However, it was not done here due to experimental limitation.

From experiment researches in glass plates [31,32], they were shown that the total integrated surface scattering and bulk scattering for glass plates were at 10^{-4} ($\sim 6 \times 10^{-4}$) level of the incident pulse. The scattering radius at 1.5° about 1 m after the glass plate is about $1000 \times 1.5 \times \pi/180 \approx 26$ mm. In the experiment, owing to the self-focusing effect, the SD1 beam diameter was about 3 mm in the distance about 1 m after the glass plate. As a result, although the scattering light mostly appears in the region closing to the incident beams, the scattered

#132521 - $15.00 USD Received 2 Aug 2010; revised 5 Sep 2010; accepted 7 Sep 2010; published 6 Oct 2010

light in the SD1 signal direction can be estimated roughly to be the area ratio between the SD1 signal and the scattering area ~$6 \times 10^{-4} \times [\pi \times (3/2)^2] / (\pi \times 26^2)$, which is at the level of ~1.8×10^{-6}. This measured enhancement of the temporal contrast is limited by the sensitivity of the spectrometer and the pulse energy in the experiment.

When the laser is nearly normal to the bulk medium, most of the surface scattering light is in the opposite direction to the transmission light. By using a bulk crystal medium, the bulk scattering is expected to be much weaker owning to low heterogeneity. In the experiment, the glass plate was located after the focal position. The SD1 signal has smaller divergence angle in compare with the scattering light. Then, the scattered light can also be reduced much more by propagating the SD1 beam for longer distance or using a spatial filter. Here, the scattering light was just considered spatially. In the time domain, does the scattering light in the SD1 signal direction have broader pulse duration than that of the prepulse and will decrease the intensity of the scattering light? How does the intensity of the incident pulse affect the scattering intensity? Detail studies are needed to figure out which parameters will affect the scattering intensity and how to eliminate the scattering intensity from the bulk medium in the future.

7. Conclusion

In conclusion, we have demonstrated the application of the self-diffraction process in electronic Kerr media for femtosecond pulses cleaning. In this method, there is no need of polarizer because the generated SD signals are spatially separated from the incident laser beams. Without the need of polarizer, this method is less cost and can be used at different center wavelength from UV to MIR which is just limited by the transmission of the bulk medium. Moreover, the temporal contrast improvement will not be limited by the extinction ratio of the polarization discrimination device which is at best 4-5 orders. It was proved that the temporal contrast can be improved by four orders of magnitude even in the picosecond time regime for the SD1 signal in the experiment. The contrast improvement here is limited by the sensitivity of the spectrometer and the pulse energy in the measurement.

Much higher improvement of temporal contrast is expected to be obtained by reducing the scattered light from the satellite prepulses and decreasing the angular dispersion of the SD1 signal. The scattered light by the bulk medium can be reduced by using a crystal medium with smaller surface roughness. This scattering can also be reduced by propagating the SD1 signal for a long distance or using a spatial filter. The angular dispersion of SD1 can also be reduced by a prism pair or a grating- deformable system. Larger improvement of temporal contrast can also be expected to be obtained by using a tandem self-diffraction process between the two generated SD1 signals.

The laser spectrum was smoothed and broadened, the beam profile and beam quality was substantially improved, and the pulse duration of the generated SD signals was reduced from that of the incident laser pulse in this process.

All these outstanding performances make the SD an extremely useful method for designing background-free petawatt laser systems in the future. The generated wavelength tunable CFWM signals at different wavelength from the incident pulses by CFWM process (or named nondegenerate SD process) [22] can be used as seed pulses for background-free high power CPA or OPCPA system. This method can also be used to optimize spatial, temporal, and spectral characteristics of a laser pulse for many other experiments, for example smoothing the spectrum and compressing the pulse for the hollow fiber compression system.

Acknowledgement

This work was partly supported by the 21st Century COE program on “Coherent Optical Science” and partly supported by the grant from the Ministry of Education (MOE) in Taiwan under the ATU Program at National Chiao Tung University. A part of this work was performed under the joint research project of the Laser Engineering, Osaka University, under contract subject B1-27. Jun Liu also thanks the support of opening funds of the state key laboratory of high field laser physics in China.

#132521 - $15.00 USD Received 2 Aug 2010; revised 5 Sep 2010; accepted 7 Sep 2010; published 6 Oct 2010